

Determining the electron energy distribution near the plasma potential in the earth's ionosphere

William E. Sharp, Paul B. Hays, James R. Cutler, and Michael E. Dobbs

Space Physics Research Laboratory, University of Michigan, Ann Arbor, Michigan 48109

(Received 15 September 1980; accepted for publication 10 October 1980)

A determination of the plasma potential using an electrostatic analyzer is described in which the potential difference between the instrument slit system and surrounding plasma is minimized. Data obtained from rocket-borne instrumentation demonstrate the viability of this technique for electron fluxes between thermal energies (~ 0.5 V) and suprathermal energies (many volts).

PACS numbers: 94.20.Dd, 52.70.Ds, 94.20.Mm

INTRODUCTION

Low energy electrons play a fundamental role in the energetics of planetary atmospheres. These electrons are produced as a result of ionizing processes in the atmospheric gases. After creation, the electrons lose their energy via inelastic collisions and elastic collisions and eventually become a part of the thermal electron population. Knowledge of this thermal electron density and its temperature as well as the energy distribution of the suprathermal electrons is desirable in order to determine the energy budget of the atmosphere.

Various types of instruments have been used on space probes to measure these quantities. Langmuir probes and planar retarding potential analyzers measure the integral distributions while cylindrical and spherical electrostatic analyzers are used to measure the differential distribution. Historically, the former pair of instruments have been used to obtain electron density and temperature information, while the latter pair have been used to obtain the distribution of suprathermal electrons. Spacecraft charging will prevent the differential analyzers from obtaining thermal data.

This paper describes a technique which will allow a differential energy analyzer to measure the complete energy distribution above several tenths of volts. The particular instrument used here, a gridless retarding potential analyser with a hyperbolic field (HARP),¹ is capable of high throughput for low-energy electrons while minimizing contact potential problems with walls. The basic element of the technique is to minimize the potential difference between the entrance face of the instrument and the surrounding plasma.

I. RESPONSE OF HARP TO A PLASMA

The geometry of the HARP as well as electron trajectories for three specific energies are shown in Fig. 1. The three solid electrodes form a body of revolution that upon application of a negative potential (ϕ_B) on the center electrode with respect to the upper and lower endcaps result in a rotationally symmetric quadrupole field. Off axis injection of the particles results in energy dispersion of the particles with a first order focus at E_A , a second order focus at E_B , and no focus for $E_0 \gg \phi_B$. It happens that the off axis injection is one of the keys to

being able to minimize the potential difference between spacecraft and plasma. A complete discussion of this instrument has been given by Shyn *et al.*²

The detector response to an isotropic electron flux is considered. The number of electrons per second, $S(E)$, delivered to the detector is

$$S(E) = \int \epsilon(E)(E)F(E)A\Omega T(E) dE, \quad (1)$$

where $F(E)$ is the source flux at the slit in electrons/cm²-sec-ster-ev, A is the area of the detector source (front slit in this case), Ω is the solid angle of the collector (angle of second orifice), $T(E)$ is the energy-dependent transmission of the instrument, and $\epsilon(E)$ is the efficiency of the multiplier for electrons. $A\Omega$ is not energy dependent, thus the quantity to be evaluated is

$$\int \epsilon(E)F(E)T(E) dE.$$

For the HARP the quantity

$$\int \epsilon(E)T(E) dE = C \cdot E_B \cdot T_p \cdot \epsilon_{E_B}, \quad (2)$$

where C is a constant, more commonly called $\Delta E/E$, T is the peak transmission at energy E_B , and ϵ is the channeltron efficiency at E_B . Defining the average flux over the transmission functions at energy E_B as

$$\bar{F}(E_B) = \frac{\int \epsilon_{E_B}(E)F(E)T(E) dE}{\int \epsilon_{E_B}(E)T(E) dE}, \quad (3)$$

then by (2)

$$\int \epsilon(E)F(E)T(E) dE = \bar{F}(E_B) \cdot C \cdot E_B \cdot T_p \cdot \epsilon_{E_B}, \quad (4)$$

and thus (1) becomes

$$S(E) = C \cdot A \cdot \Omega \cdot T_p \cdot E_B \cdot \epsilon_{E_B} \cdot \bar{F}(E_B). \quad (5)$$

The count rate of the instrument is the product of $S(E)$ and the integration time, τ , of the counter. Thus

$$\bar{F}(E_B) = \frac{\text{count rate}}{\tau \cdot C \cdot A \cdot \Omega \cdot T_p \cdot E_B \cdot \epsilon_{E_B}}. \quad (6)$$

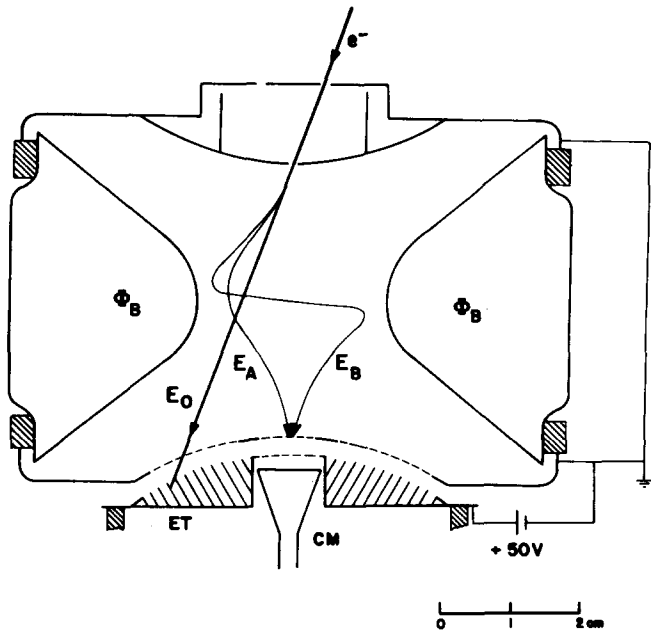


FIG. 1. Three electron trajectories with energies $E_B < E_A < E_0$ in the potential field of the HARP. ϕ_B is a negative potential for electrons. The 1st order focus is for energy E_A and is the primary focus. ET is an electron trap and CM is a channeltron multiplier.

This flux of electrons at the instrument slit plane is related to the isotropic surface flux per unit area, $J(E_B)$, being emitted from the hemisphere immediately above the slit by

$$J(E_B) = \pi F(E_B).$$

The front slit of the HARP will not be at the plasma potential in as much as any object immersed in a plasma will acquire a charge state. This is particularly true for space probes. The relationship between the fluxes at the slit and in the ambient plasma can be found by use of Liouville's theorem. This states that the density of states in phase space is constant along a dynamical trajectory. This flux of electrons at the slit, $J(E_B)$, is related to the flux of electrons in the plasma, $J(E)$, by

$$J(E) = J(E_B) \frac{E}{E_B}, \quad (7)$$

where E_B is the electron energy at the slit, and E is the energy in the ambient plasma.

Now it is necessary to find a relationship between E_B and E . The net potential on the slit will be denoted by $e\phi_0$. There are three cases to consider.

Case 1. $e\phi_0 = 0$, then $E_B = E$.

Case 2. $e\phi_0 > 0$. (8)

If α is the angle of entrance to the slit, then the geometry of the entrance aperture allows three domains to be considered for electron entrance. These domains describe electrons moving away from the slit surface, parallel to slit surface, and toward the slit surface. An analysis of the velocity components yields the following expressions for the energy at the slit.

Domain $E_B < e\phi_0$, $E_B = (e\phi_0 - E)/\cos 2\alpha$. (9)

Domain $E_B = e\phi_0$, $E_B = E/\sin^2 \alpha = e\phi_0/\cos^2 \alpha$. (10)

Domain $E_B > e\phi_0$, $E_B = E + e\phi_0$. (11)

Equation (9) expresses the fact that electrons initially traveling away from the slit are pulled back into the slit. Equations (10) and (11) express the fact that electrons traveling parallel to the slit and toward the slit are accelerated to the slit. Thus their energy is greater at the slit surface than in the ambient plasma.

Case 3. $e\phi_0 < 0$.

The geometry of the entrance aperture, for $\alpha \neq 0$, allows only one possibility for electron entrance.

Domain $E_B > e\phi_0$, $E_B = E - e\phi_0$. (12)

Figure 2 illustrates the domains of these functional relationships. Consequently, in calculating the $J(E)$ from (6) and (7) the condition of $e\phi_0$ and the domain must be ascertained. The appropriate expression for E is then placed in (7) and the flux calculated.

II. THE SEARCH MODE

Spacecraft immersed in the ionosphere/plasmasphere generally have a potential $e\phi_s$, of a negative 1–3 V. On some occasions, particularly with satellites, the potential can be considerable; for example, several volts to kilovolts on ATS-5³ and ATS-6.⁴ The absolute energy basis of the sampled electrons depends upon the knowledge of the spacecraft charge state. Active control of the spacecraft potential at a very low or zero potential value can ensure that all low-energy particles are sampled by the instrument. For charge states between ± 5 V a method has been designed and tested to measure the potential. This method is based upon the intrinsic feature of the sensor in which the instrument reference potential is servoed to compensate the spacecraft potential.

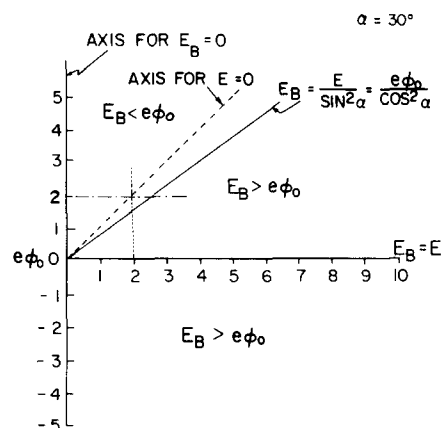


FIG. 2. The domains for the functional relationships between the net potential on the entrance slit, $e\phi_0$, and the potential on the central electrode, $E_B = e\phi_B$. The dotted line describes holding E_B constant and varying $e\phi_0$ while the dot-dash line describes holding $e\phi_0$ constant and varying E_B .

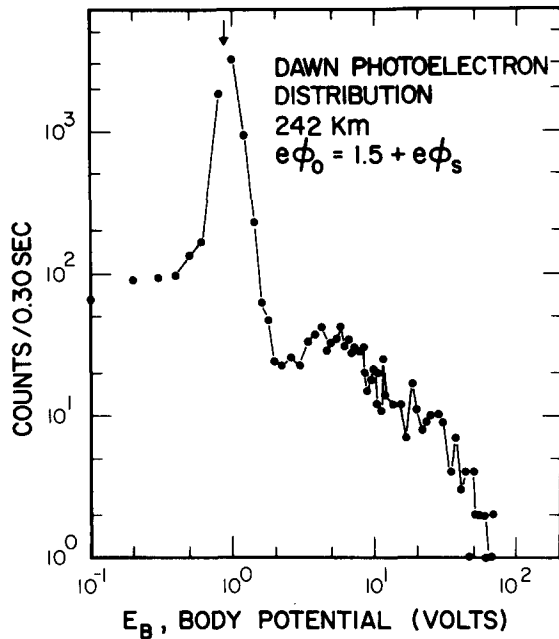


FIG. 4. Count rate of multiplier vs changing E_B when $e\phi_0$ is constant ($e\phi_s$ assumed constant during sweep) for a measurement of photoelectron distribution at dawn at 242 km altitude. Arrow indicates the plasma zero reference.

The scheme can be explained by the response of the sensor to an isotropic source spectrum, $J(E)$. As described in the previous section the number of electrons entering the detector is given by the functional relationship

$$S(E)(\text{electrons/s}) \propto \frac{A\Omega}{\pi} \Delta E \frac{J(E)}{E/E_B}.$$

Referring to the $e\phi_0 > 0$ domain in Fig. 2, between $E = 0$ and $E_B = E/\sin^2\alpha$ there are no electrons entering the instrument. There is a sharp transition in the number of electrons reaching the detector at exactly $E_B = e\phi_0/\cos^2\alpha$ [Eq. (10)] followed by decreasing counts. Consequently, one can fix the selection energy, $E_B = e\phi_B$, relative to the instrument reference potential, $e\phi_c$, and find the transition by sweeping this reference potential from positive toward negative voltage (the dotted curve in Fig. 2) while monitoring the output. The transition is a very steep function of reference potential at which

$$e\phi_0 = e\phi_B \cos^2\alpha. \quad (13)$$

The net potential is composed of the spacecraft potential and an applied potential,

$$e\phi_0 = e\phi_c + e\phi_s, \quad (14)$$

thus

$$e\phi_s = e\phi_B \cos^2\alpha + e\phi_c. \quad (15)$$

Since ϕ_B is preselected, α determined by the geometry of the slits and ϕ_c a known variable, the plasma potential

ϕ_s is uniquely determined. Correcting the reference potential for this plasma potential then allows the low-energy electrons near the plasma potential to enter the detector. They would be forbidden entrance otherwise.

An alternate way of finding the transition is to apply a reference potential in excess of an estimated plasma potential and sweep the body potential with respect to the reference potential (dot-dashed curve). The arguments from Eq. (13) still apply.

III. INSTRUMENT LOGIC

A block diagram of the instrument with the electronics to do the logic described by Eqs. (13)–(15) is shown in Fig. 3. The sweep potential generator, reference potential generator, and the logic that runs them will be briefly discussed.

The ϕ_B generator provides the sweep voltage to the analyzer to select the desired electron energy. 0–100 V and 0–1000 V ranges are provided, as well as, fixed potential for ϕ_c search. The output is referenced to ϕ_c to maintain constant focusing fields in the analyzer regardless of the reference potential. The sweep shape is identical between ranges. ϕ_B is simply scaled by ten to change ranges. The ϕ_B generator has four major sections: the sweep index counter, PROM sweep shaping, the digital to analog converter, and the output amplifier.

A 7-bit sweep index counter is reset at the beginning of each sweep and is incremented between each energy level measurement interval. Reset and increment signals are provided by the instrument sequence logic.

A 64 word by 12 bit programmable read-only memory provides the desired sweep as a function of sweep index number. The sweep magnitude output values are chosen to complement the constant $\Delta E/E$ characteristic of the analyzer with small differences between small outputs and the difference between steps increasing with step number.

A 12-bit digital to analog converter converts the magnitude number to between 0–10 V with a resolution of 0.0025 V per bit with about 1.25 mV accuracy. This translates to 12.5 mV accuracy on a 100 mV sweep step (or 125 mV accuracy on a 1 V sweep step in the high-energy sweep mode).

The output amplifier has a programmable gain of –10 v/v or –100 v/v from the D to A output to produce the 0–1000 V ϕ_B sweep, respectively. The ϕ_c digital to analog converter output is added with constant gain in order to reference the ϕ_B to ϕ_c .

The reference potential applied to the front plate, ϕ_c , is provided by the ϕ_c generator. The ϕ_c for each spectral scan is determined either automatically by a bias search or is commanded to a prescribed value. In the automatic mode prior to each scan ϕ_B is preset to –1 V and ϕ_c is swept from +5 toward –5 V in 50 mV steps until a large decreasing count is reached in the data accumulator and the ϕ_c value at this point plus an offset is applied to the front plate for the subsequent spectra. If the decreasing count is not reached as might be the

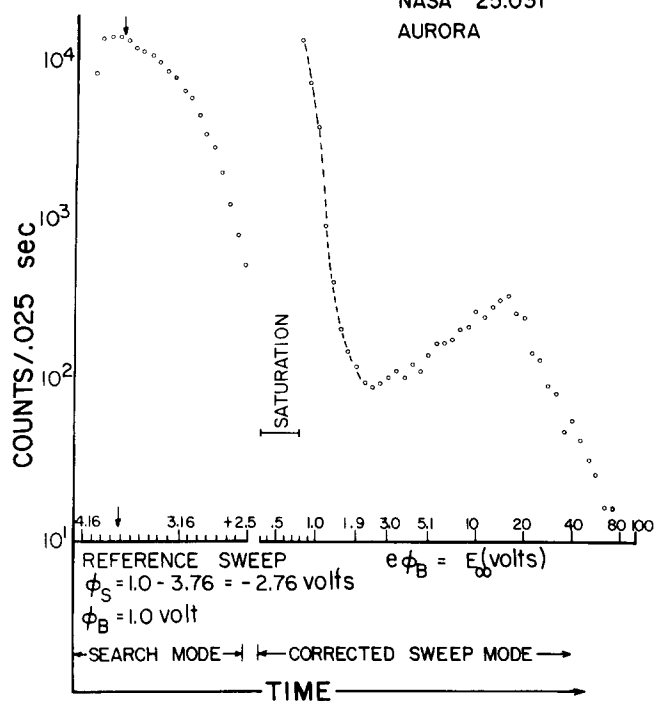


FIG. 5. Count rate of multiplier vs changing $e\phi_0$ when E_B is constant for search mode. Vertical arrow identifies plasma zero reference. E_B ($\approx E_x$) is changed for the corrected reference potential in the corrected sweep mode.

case in very low plasma densities, or a vehicle whose charge state is outside the measurement range, the preset value is used during the following energy sweep. The generator has four major sections: the bias index counter, the digital to analog converter, the output amplifier, and the bias search logic.

The 8 bit bias index counter is either preset to the commanded bias or reaches a value under control of the bias search logic. In the search mode the counter steps at 2 KHz.

A 10-bit digital to analog converter converts the bias index to between -10 and $+10$ V with a resolution of 0.08 V per bit with about 10 mV accuracy. This corresponds to at least 6.25 mV accuracy in ϕ_c .

The output amplifier has a gain of -0.66 v/v from the D to A output to produce the $+5$ – -5 V ϕ_c as required. The ϕ_c offset for search purposes is introduced here.

In response to a sweep initiate signal the bias control logic resets the bias index counter (ϕ_c to $+5$ V) and resets the sweep index counter (ϕ_B to -1 V). The data accumulator is zeroed and enabled to count continuously. The bias index counter is incremented at 2 KHz causing ϕ_c to sweep from $+5$ V toward -5 V in 50 mV steps.

When the difference between succeeding counts is positive the bias index counter value is saved until the search period is complete. The ϕ_c value, less 1 V, is then held fixed for the spectrum measurement interval. If the bias index counter overflows (at -5 V) the automatic system is out of range and a predefined bias value is used.

IV. TEST RESULTS

The verification of these concepts has been accomplished by carrying sensors on several rocket flights over the past few years. Figure 4 shows the resulting data when the applied fixed reference potential exceeded the plasma potential. In the energy region less than 0.8 V, the electrons initially moving away from the sensor (in part due to scattering off the face of the sensor) are drawn back in. Between 0.8–1.0 V the plasma potential region is crossed (vertical arrow). Following that the count rate decreases dramatically characteristic of the Maxwellian distribution of the thermal electrons. A distribution temperature can be deduced from the slope.⁵ At higher energies the count rate distribution takes on the form characteristic of the photoelectrons in the dawn atmosphere.¹

Figure 5 illustrates the results for a flight where the logic of the flight instrument (discussed in the previous section) identified the plasma potential (vertical arrow) during a reference potential sweep with the central electrode at a fixed potential of 1.0 V. Note that the identification is made by the decreasing count. Because of the entrance angle of 15° and the central electrode potential of 1.0 V, the energy width of the region for no electron entrance was only 70 mV. The step size on the reference potential sweep here was 75 mV and the instrument resolution at 1.0 V was 150 mV. Thus the void region would be masked and only a decreasing count would give evidence of having passed the plasma zero point. The reference potential of decreasing count was stored (3.76 V here) and subtracted from the 1.0 V central electrode potential giving a plasma potential of -2.76 V. The reference potential was then set to $+2.76$ V and the central body potential was swept from 0.3 V–100 V. This would essentially be the ambient energy of the electrons. Since this new reference potential was very near the plasma potential, the detector saturated due

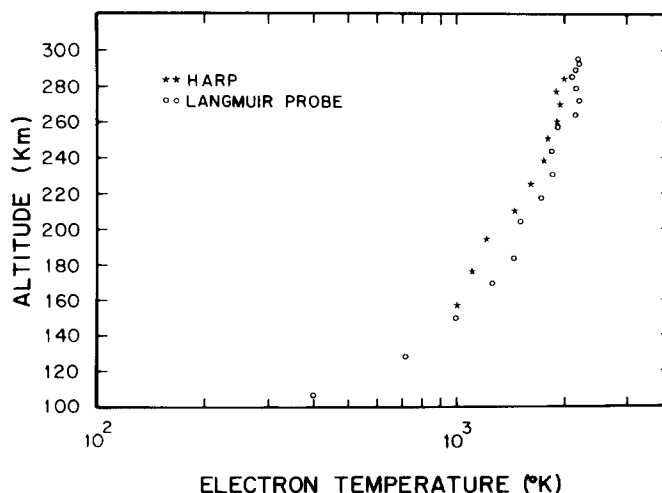


FIG. 6. Electron temperature, T_e , deduced from HARP measurements and Langmuir probe measurements on same flight.

to the large fluxes of thermal electrons below 0.8 V. Note, however, the rapid decrease in count rate above 0.8 V. This is characteristic of the Maxwellian distribution and a temperature for the distribution can be deduced from the slope.

A comparison between the electron temperatures found during a flight in which the HARP and a Langmuir probe were both on the payload is given in Fig. 6. These data were obtained on the flight which gave the data of Fig. 4.

ACKNOWLEDGMENT

This work has been supported by NASA Grant NGR 23-005-360.

- ¹ P. B. Hays and W. E. Sharp, *J. Geophys. Res.* **78**, 1153 (1973).
- ² T. W. Shyn, W. E. Sharp, and P. B. Hays, *Rev. Sci. Instrum.* **47**, 1005 (1976).
- ³ S. E. De Forest, *J. Geophys. Res.* **77**, 651 (1972).
- ⁴ E. C. Whipple, *J. Geophys. Res.* **81**, 715 (1976).
- ⁵ P. B. Hays and A. F. Nagy, *Planet. Space Sci.* **21**, 1301 (1973).